Environment and Natural Resources Journal

Volume 22
Issue 2
2024

Fine Scale Modeling for Potential Distribution of Dengue Fever in Tampan District, Indonesia

Eggy Arya Giofandi[1*] Dhanu Sekarjati[2], Cipta Estri Sekarrini[3], and Yuska Nelva Sari[4]

[1]Graduate Program of Regional Planning Science, Faculty of Agriculture, IPB University, West Java 16680, Indonesia
[2]Geoinformatics, Department of Computer Science, College of Computing, Khon Kaen University, Khon Kaen 40000, Thailand
[3]Doctoral Program of Geography Education, Faculty of Social Science, Universitas Negeri Malang, East Java 65145, Indonesia
[4]Pekanbaru City Health Office, Riau Province 28288, Indonesia

ARTICLE INFO

Received: 24 Jul 2023
Received in revised: 31 Dec 2023
Accepted: 17 Jan 2024
Published online: 5 Feb 2024
DOI: 10.32526/ennrj/22/20230196

Keywords:
Epidemic/ Kernel-density estimation/ Neighboring algorithm/ Surveillance/ Tampan District

*** Corresponding author:**
E-mail: eggyarya@apps.ipb.ac.id

ABSTRACT

Larvisiding is one common way used to reduce mosquito density in breeding areas before metamorphosizing into adults. Despite numerous eradication efforts, the outcomes have not met expectations, leading to additional issues such as environmental pollution in urban areas. In the context of dengue hemorrhagic fever (DHF), addressing the challenge of mitigating the endemic outbreak entails formulating an effective strategy through a vector eradication approach. Therefore, this study explored the spatial pattern of DHF and estimated the potential spread of outbreaks. A geographic information system approach, with nearest neighbor analysis and kernel density estimation (KDE), was used to generate information regarding the pattern and potential for transmission of *Aedes aegypti* mosquitoes. The results showed that in 2019, a random pattern was observed, while in 2020, a clustered pattern of virus spread occurred. Furthermore, in terms of the potential transmission, an exposed zone of 9.73 km² was identified in 2019, and this increased to 15.72 km² in 2020. In this study, several important actions were implemented with a spatial approach, enabling the detection and polarization of events. However, the limitations included not being comprehensive in addressing the hygiene, sanitation, drainage, and population density aspects.

1. INTRODUCTION

Dengue hemorrhagic fever (DHF) is a seasonal disease, posing an unresolved health issue with significant social and economic dimensions. The spatial connections to environmental aspects, particularly cleanliness, play a crucial role in the impact of DHF outbreaks (Lawson and Williams, 2001). Efforts to reduce disease transmission have been undertaken by various scientific groups with diverse perspectives, but the results obtained have not been optimal (Sekarrini et al., 2022a). The estimation of transmission through *Aedes aegypti* mosquitoes is derived from patient data history associated with the population, collected from health agencies. The detailed tracking of the population has been recorded and is assumed as the basis for calculating transmission cases (Firdous et al., 2017).

The rapid spread of the virus over 2-7 days is facilitated by the movement of *Aedes aegypti* mosquitoes, resulting in symptoms such as high fever, weakness, and red spots on the skin (Murray and Smith, 2013; Sekarrini et al., 2020). The transmission is enhanced by environmental conditions characterized by minimal vegetation, low transportation density, lowlands, and rapid urban development, allowing for the uncontrollable proliferation of *Aedes aegypti* mosquitoes (Hii et al., 2012). This information is also substantiated by the impact of anthropogenic growth on the natural environment, leading to various issues concerning ecosystem damage (Wijayanti et al., 2016). The measurement of DHF outbreak transmission can be conducted using a mapping tool derived from the results of transmission detection, incident detection,

Citation: Giofandi EA, Sekarjati D, Sekarrini CE, Sari YN. Fine scale modeling for potential distribution of Dengue Fever in Tampan District, Indonesia. Environ. Nat. Resour. J. 2024;22(2):105-118. (https://doi.org/10.32526/ennrj/22/20230196)

and prevention coverage implemented by health agencies (Rushton, 2003; Waller and Gotway, 2004; Sekarrini et al., 2022b). The effect of weather variables on the magnitude of dengue fever distribution has been established in several previous studies. These studies explored changes in infectivity and vector survival rates, showing the sensitivity of climatic factors to dengue transmission (Negev et al., 2015). Furthermore, the lack of sanitation, poor activity patterns, declining water quality, and existing health conditions interact with the growth of *Aedes aegypti* mosquito vector, forming a common challenge in relation to the prevention and control of DHF (Devine and Furlong, 2007; Bansal et al., 2011).

The impact of DHF transmission on health investigations is reflected through the utilization of geographic information systems methodologies (Giofandi et al., 2023). Scientific application of geographic information systems enables the determination of a case location and the assessment of its influence pattern on the surrounding area (Gatrell and Luytonen, 2003). The role of geographic information systems in managing and analyzing environmental health surveillance data is recognized as changes are occurring in the presentation of information in the field of public health. Furthermore, the potential for DHF transmission through the bite of *Aedes aegypti* mosquitoes can be estimated using the kernel density estimation (KDE) approach. This approach uses a calculation technique based on the relative location of incidents through spatial devices, considering various environmental aspects. The results can be applied to policy and interactive planning of event estimates to address the increased population activity associated with transmission (Spencer and Angeles, 2007; King et al., 2016). The KDE algorithm, with locations monitored at high spatial resolution and population incident data, produces a favorable output for the development of a spatial transmission method based on field observation. In this context, the problem of modifiable unit area is addressed by associating each event with a fixed zone setting (Arifin et al., 2016). The challenge in implementing KDE lies in the selection of parameter clusters, enabling the adaptation of network density settings for problem-solving.

In the western part of Indonesia, dengue fever issues based on a geospatial approach are seldom addressed by a few studies. In most cases, global assessments are the main focus, with less attention given to crucial problems at a more detailed level. The utilization of surveillance data for local observations is one of the calculations used to estimate the future incidence of dengue fever, in line with the Sustainable Development Goals (SDGs) program. Pekanbaru City is one of the urban areas with the highest incidence of dengue fever cases. The characteristics of lowland areas, with an altitude of <100 meters above sea level, increase the prevalence of *Aedes aegypti* (Molina et al., 2022), The similarity in these topographic conditions is one factor in selecting the Tampan District as an observation area. In recent periods, an increase in built-up land in urban areas without corresponding improvement in sanitary environmental conditions and drainage channels has led to a higher potential for the presence of *Aedes aegypti* mosquito habitats (Liu et al., 2022).

This study aimed to determine the spatial pattern of dengue fever incidence and estimate the potential spread of outbreaks. The spatial pattern of incidence was identified using nearest-neighbor analysis in the form of clusters. This part is essential for representing the regional intensity of dengue fever incidence within the cluster. To estimate the potential for transmission, geographic information system (GIS) techniques through a KDE approach were used. Public health resources continue to be burdened by the incidence of this epidemic, and the transmission of DHF changes dynamically, necessitating more effective monitoring and control strategies. Therefore, this model is expected to provide a better understanding of DHF incidence problem. It can also be implemented as one of the approaches at the urban scale, specifically in areas with morphological conditions and other aspects similar to sustainable development.

2. METHODOLOGY

2.1 Study area

This study was conducted at the Tampan District of Pekanbaru City, located in the center of Sumatra Island, Indonesia, as illustrated in Figure 1. Geographically, the observation area is situated at 101°22'45"-101°23'09" East Longitude and 0°28'41"-0°29'09" North Latitude, covering an area of 57 km^2 and falling within a densely populated region. One of the primary reasons for selecting this location is the relatively flat to undulating topographic conditions and high air humidity, reaching 89%. In addition, this area is known for having a high potential for dengue fever cases, as shown by recent reports.

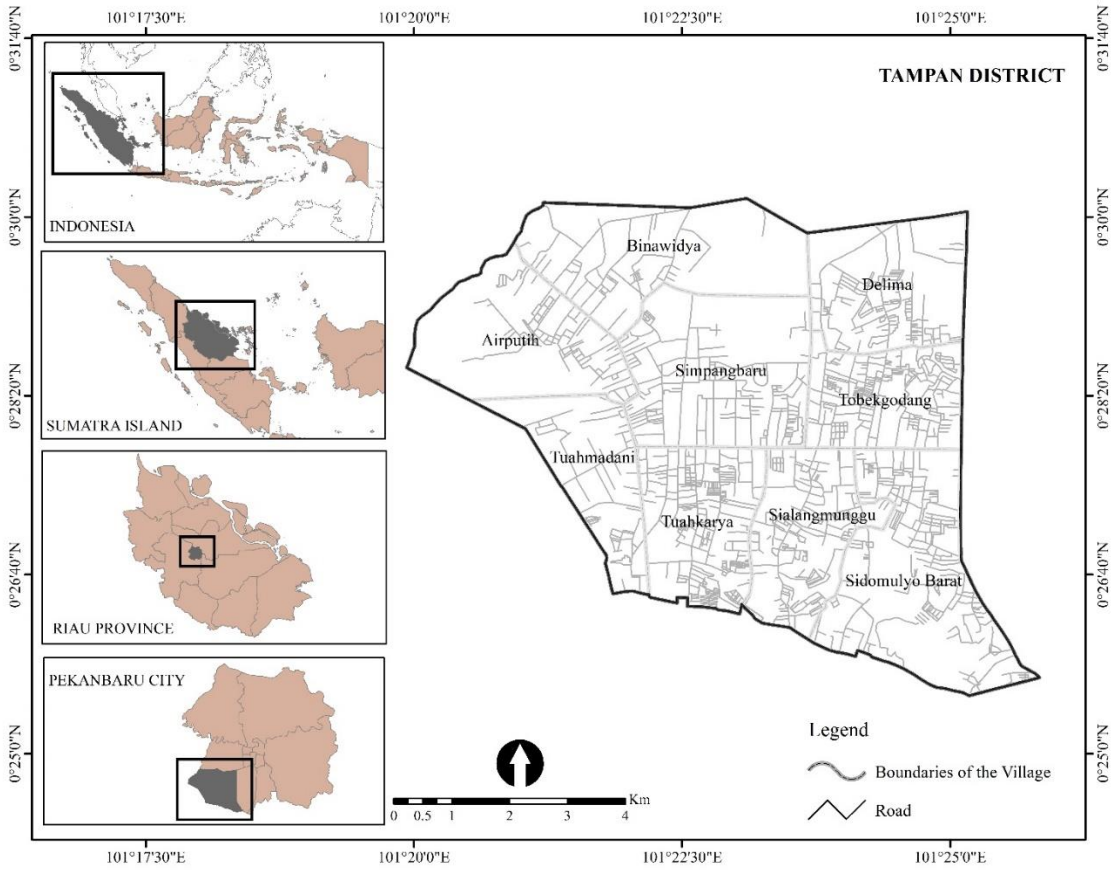

Figure 1. Study site

2.2 DHF epidemiological data

Monthly reports of dengue fever cases were collected from the surveillance database of the Riau Provincial Health Office representative in Tampan District, Pekanbaru City. Monthly dengue incidence reports from nine villages were observed from January 2019 to December 2020. The surveillance system data were initiated from reports by hospital inpatients, health centers, and pharmacies, which were then detected by officers. The report did not include information on the burden of infection and manifestations of dengue fever but provided the coordinates of the residence and age of patients (Table 1). Therefore, reports confirmed by health agency officials were used in this study, and all the data were spatially processed using the nearest neighbor statistical index and kernel density estimation (KDE). All processing was carried out with the Spatial Statistics and Geographic Information Systems (GIS) software (Figure 2).

Table 1. Age categories of patients infected with *Aedes aegypti* mosquitoes

Age group	Category	2020	(%)	2019	(%)
<5	Toddler	4	0.05	3	0.10
6-11	Childhood	8	0.10	6	0.20
12-16	Early Adolescence	13	0.16	6	0.20
17-25	Late Adolescence	29	0.36	6	0.20
26-35	Early Adulthood	14	0.18	2	0.07
36-45	Late Adulthood	8	0.10	4	0.13
46-55	Early Old Age	1	0.01	2	0.07
>55	Late Old Age	3	0.04	1	0.03
	Total	80	1.00	30	1.00

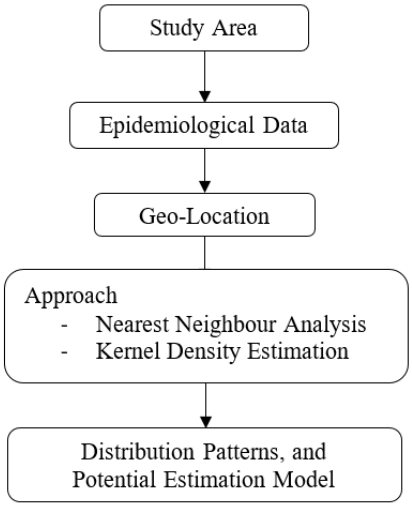

Figure 2. Flow chart of the methodology

2.3 Detection of incidence distribution and potential transmission of *Aedes aegypti*

The processing carried out to detect clusters of distribution linkages between incident locations aimed to discover distribution patterns and help filter out irrelevant information. The neighboring statistical algorithm used to detect the distribution pattern of Dengue hemorrhagic fever (DHF) incidence was calculated using the formula:

$$R = Ju/Jh \quad (1)$$

Where; R is the target, Ju is the average observed distance between each object to be measured, and Jh is the expected distance in a distribution. This analysis required data on the distance between one settlement and another, considered a point in space used to assess the spread pattern of geographical phenomena. Furthermore, the estimation of potential transmission considered the flying capabilities of mosquitoes with an average of 50 meters to 50 km, depending on the species. The migration range of mosquitoes significantly influences the ecology and physiology of the species, irrespective of the disturbance situation. When the flight is related to disturbance, the species tend to cover shorter distances ranging from 25 meters to 6 km^2 (Verdonschot and Lototskaya, 2014).

In the context of *Aedes aegypti* mosquitoes, the flight distance was estimated to be about 400 meters (Satoto et al., 2019). The relatively simple formula for KDE was used with a conceptual method that could be simplified according to the phenomenon under examination. The application of physics analogies could be used to understand how the density estimation kernel works. The algorithm for KDE in determining potential areas for DHF outbreaks was calculated using the formula:

$$f(x) = \frac{1}{nh} \sum_{t}^{n} = 1K\left(\frac{X - Xt}{h}\right) \quad (2)$$

$$K(x) = \frac{3}{4}(1 - x^2), |x| \leq 1 \quad (3)$$

$$\text{Bandwidth} = 0.9 * \min\left(SD, \sqrt{\frac{1}{\ln(2)} \times Dm}\right) \quad (4)$$

Where; h is the bandwidth, n is the number of cases, X-Xt is the distance from the center of the incident, and K is the quadratic kernel function of the equation. Bandwidth refers to the shorter value of the height from the output level in a spatial reference (Sun et al., 2019). Meanwhile, the bandwidth value of the standard distance has been derived from SD of the distance between each point. Dm is the medium distance value of the point distribution pattern (Wang et al., 2019).

Vector formats are used majorly for making disease maps based on aggregated data but the major drawback is the limited availability of detailed disease case data. This is important because data acquisition is subject to high subjectivity and low precision (Shi, 2010). To overcome these challenges, a KDE simulation was conducted to cover multi-modal distributions with minimal errors. In this study, one circle of data was uniformly randomized from a uniform distribution, incorporating either normal bivariate distribution or a combination of two or three. The density value function can estimate the excess of points or compare to the underlying value of each point (Donthu and Rust, 1989).

The results between boundary coverage and geolocation of Point of Interest (POI) events were assessed to understand the rationality and traceability effectiveness of the kernel density estimation approach. The area within the POI with high estimation potential was considered to have the most frequent transmission. Therefore, the calculation of the accuracy was based on a precision indicator, which entailed dividing the delimited area by the identical area and multiplying the result by 100%. This value was used in the process of calculating the area ratio of points found within the radius of the incident POIs.

3. RESULTS AND DISCUSSION

3.1 Distribution of DHF patients

This study focused on location information, specifically the proximity or distance of an activity from the surroundings. Location information in this study was conducted to discover the distribution of Dengue hemorrhagic fever (DHF) events which was limited by an administrative scale, namely Tampan District, Pekanbaru City with spatial distribution patterns of incident locations through statistical analysis of nearest neighbor.

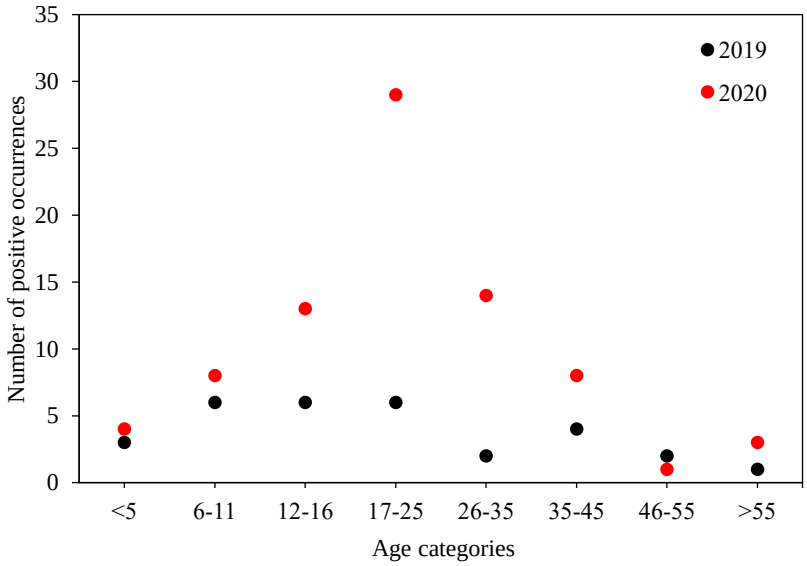

Figure 3. Age distribution of patients with DHF incidence in Tampan District

Based on the results, patients infected with *Aedes aegypti* mosquitoes varied, with a dominance of late adolescence to children (six cases each), in 2019. Meanwhile, in 2020, most patients were found in the age category of early adulthood to adolescence, between 17-25 years, as shown in Figure 3. Therefore, it is recommended that the surveillance of virus transmission age in the Tampan District be further strengthened, and a highly sensitized emergency response to control transmission be established. The continued implementation of health education programs focused on infectious diseases at the school level and suitable for both children and adults is also essential (Portella and Kraenkel, 2021). The results further showed that the peak period for acute infectious diseases in the Tampan District was between June to December, coinciding with the rainy season in the island of Sumatra, Indonesia. Moreover, a more responsive tracking system in the specific identification process can minimize potential breeding sites, contributing to the prevention and control of mosquito habitats (Zhang et al., 2023).

Information related to the distribution pattern of DHF sufferers was measured by the statistical value of the nearest neighbor index, ranging from 0 to 2.15. Values approaching 0 are included in the category of clustered pattern, while those approaching 2.15 are identified as a uniform pattern. An index value of 1.0 positioned in the middle, suggests a random pattern without bias toward clustering or uniformity.

The statistical calculation of the nearest neighbor index for the location of the patients in 2019 yielded a value of 1.0622. A total of 30 location points were identified, forming the second quadrant with a random distribution pattern. This spatial information is evident in the irregular pattern represented by the yellow 1-point figure, which separates from the surrounding locations. Meanwhile, the nearest neighbor statistical index value for events in 2020 was estimated at 0.6505. A total of 80 location points were identified, forming a clustered distribution pattern. When observed spatially, these incidents form a clustered pattern, as illustrated in Figure 4. Information related to the pattern of incident groups includes proximity among certain locations, suggesting a potential vulnerability in the transmission of DHF. The results were consistent with a study conducted in other Southeast Asian countries where the highest incidence occurred in the productive age, attributed to climatological conditions (Masrani et al., 2022). Some estimates of increased vector transmission occur during the journey to school or work (Ragab et al., 2023).

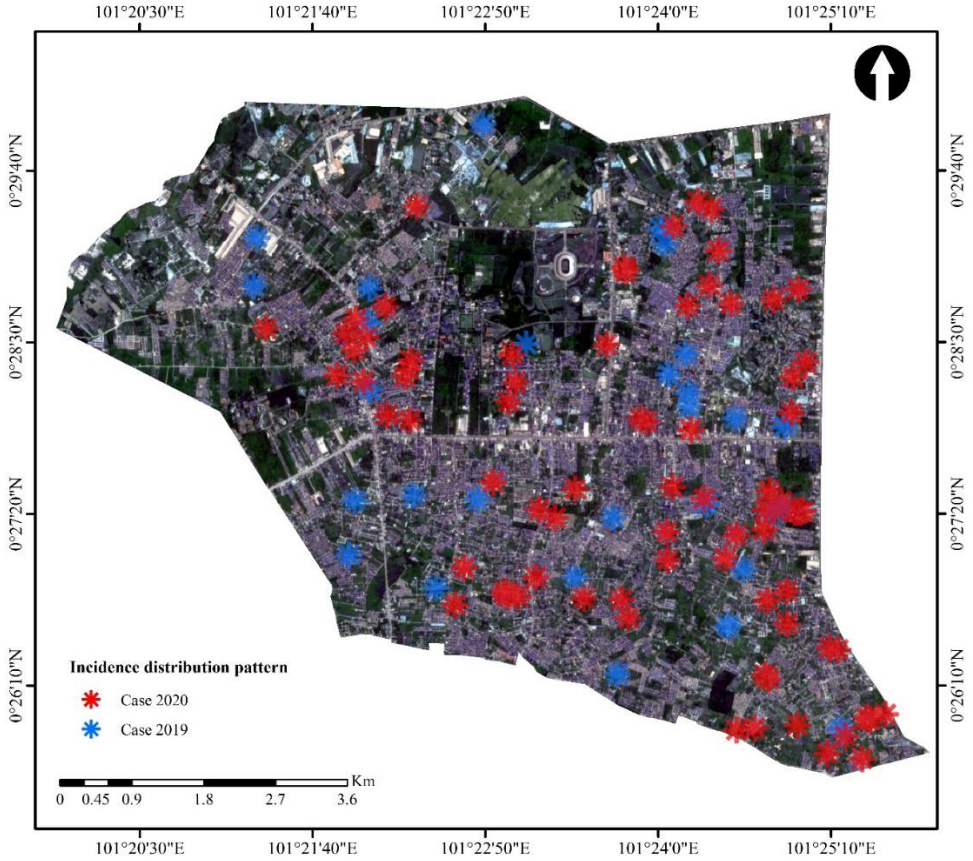

Figure 4. Distribution pattern in 2019 and 2020

The 2019 nearest neighbor statistical index value is marked in yellow, representing a random pattern category. Meanwhile, data obtained from the nearest neighbor statistical index value for 2020 showed a clustered pattern marked in blue (Figure 5). Information regarding the condition of the house and the surrounding environment is needed in structured and visual analyses to determine the conditions of *Aedes aegypti* mosquito habitats.

These results were corroborated by data from the surrounding climatological station detailed in the yearbook, indicating a significant increase in surface temperature from 2020 with an average temperature of 28.83°C to 34.80°C in 2021 (SoPM, 2021). This increase enhances the suitability for the existence of *Aedes aegypti* mosquitoes as also described by (Lubinda et al., 2019) who identified the most suitable temperature range for the environmental habitat to be 28-35°C. Another study (Setiawati, 2019) stated that urban development provided an expansion of movement for dengue vectors including *Aedes aegypti* and *Aedes albopictus* mosquitoes. Response variables such as climate factors were reported to affect the incidence of dengue fever by 66.1%. The peak of the strongest variable was found from rainfall followed by the surface temperature. The presence of *Aedes aegypti* larvae adapts well to poor water and overpopulated areas, effectively breeding in such habitats (Ramadona et al., 2023).

The observed change pattern was attributed to extreme temperature changes resulting from increased greenhouse gas emissions, deforestation, sea level rise, and global warming. Although environments with increased temperatures are more prone to *Aedes aegypti* mosquitoes (Ferraguti et al., 2023), current conditions are reducing the distribution, leading to adaptive clustering.

3.2 Potential of *Aedes aegypti* transmission

Clustering of potential transmission was performed through KDE and data types used in the analysis were derived from the coordinates of event location, categorized by sex ratio (Figure 6) and age category (Figure 8). The primary analysis of potential transmission through statistical estimation illustrated the influence of high infection density during the observation year. Therefore, this area should be considered when planning strategic actions for incidence control in anthropogenic activity land use areas.

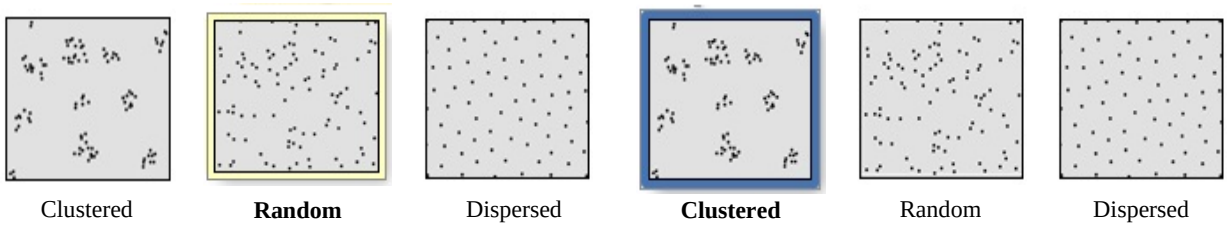

Figure 5. The results of the closest neighbor analysis pattern in 2019 and 2020

The KDE showed the existence of a centralized dengue transmission location and the calculation was based on the sex ratio for 2019 and 2020, as shown in Figure 6. Significant movement was observed among females in 2020, totaling 38 incidents, while groupings were formed in several parts for the movement of transmission events based on the male gender, reaching 42 incidents (Figure 6(a)). In the female gender, transmission occurred widely and randomly, as observed from the movement of the incidence in 2019. In 2020, this transmission occurred in clusters represented in blue (Figure 6(b)). Each result of KDE not only describes the orientation of the incident locations during the observation period but also shows valuable insights for surveillance surveyors to respond promptly to ongoing events.

The analysis showed that based on the sex ratio, the risk of transmission was higher in females compared to males. These results are expected to aid in the identification of populations in vulnerable areas and in conducting early diagnoses for appropriate treatments to reduce the number of incidents, specifically in females. In general, the total vulnerable area observed increased for both male and female incidents, as shown in Figure 7. The potential area for the male gender increased significantly from 6.65 km^2 to 15 km^2. Within the <100-meter range, the area increased by 76 hectares, in the 100-200-meter range, there was a rise of 200 hectares. Furthermore, in the 200-300-meter radius, there was a broader expansion of 263 hectares, and in the farthest 300-400-meter radius, the increase amounted to 296 hectares.

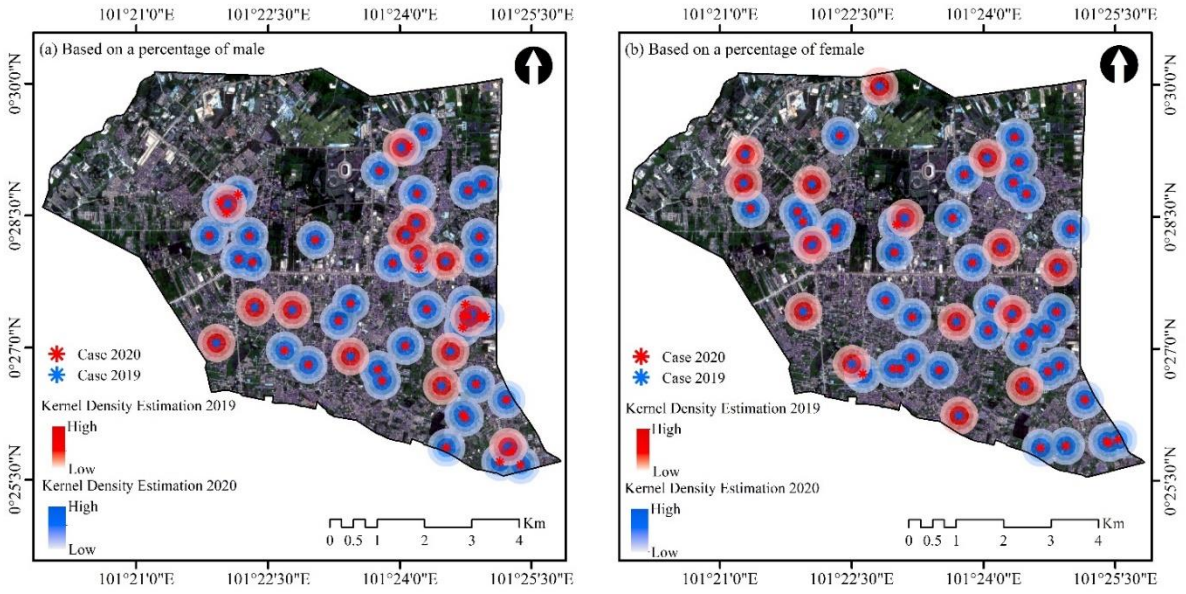

Figure 6. Kernel density estimation based on gender ratio in 2019 and 2020

The incidence rate in females was found to also increase but not significantly compared to males. This was observed in the rise from 7.31 km^2 to 7.47 km^2 in 2019 and further to 14.78 km^2 in 2020. The observation was grounded in the proximity of transmission events and the influence of climatology, which shortened the range of mosquitoes. The estimated area of the exposed zone in the <100-meter radius increased to 69 hectares, the 100-200-meter radius covered 181 hectares, the 200-300-meter radius had a coverage area of 237 hectares, and the farthest radius of 300-400 meters resulted in a reachable area

of 244 hectares. Furthermore, the KDE approach was used to assess the eight age categories. This consideration was used to determine the number and distribution of events in each age grouping of patients infected with *Aedes aegypti* mosquitoes.

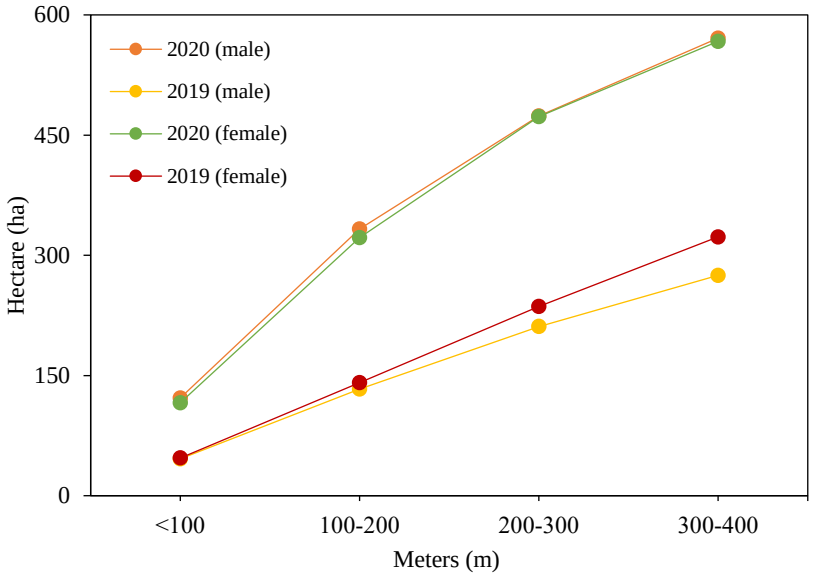

Figure 7. The curve of DHF spread based on gender ratio in 2019 and 2020

In general, the total incidence of dengue fever varied in age categories from Early Adolescence to Early Adulthood (Figure 8). In this age category, individuals are in the productive age, actively engaging in daily activities, while fewer cases were found in the growing age group. This was illustrated in Figure 8(a) and (b), respectively, showing an increase in cases with the incident initially changing randomly to a clustering pattern. As explained previously, the flying range and the presence of wind acting as factors affecting movement speed contribute to mosquito transmission occurring in closer proximity. This phenomenon was also observed in vulnerable age groups such as the Early Old and Late Old, where transmission movement activities occurred far apart, potentially starting with the presence of new breeding habitats. Furthermore, the Late Adolescence group was identified as the most vulnerable age for dengue fever transmission incidents. This result is evident in Figure 7(d), which interprets the movement of *Aedes aegypti* mosquitoes from the previous year. It was found that almost all incidents had intersections with the year 2020, creating a pattern of incidents occurring in close proximity, and designating this area as a red zone. The estimated transmission in 2020, represented by blue, overlaps with that of the previous year. When interpreted more broadly, the potential for incidents in the following year did not change significantly within the transmission area.

Various age categories were considered to determine the potential transmission of dengue fever outbreaks. When examined individually, specifically in the Toddler age category (<5 years), an initial random pattern of occurrence was observed, later shifting into groups. The potential coverage area varied, starting from a radius of <100 meters with an area of 13 hectares, to 37 hectares at 100-200 meters, 55 hectares at 200-300 meters, and 73 hectares at the farthest radius in 2020. In the previous year, smaller areas were observed in the potential range, namely 9 hectares for a radius of <100 meters, 28 hectares at 100-200 meters, 47 hectares at 200-300 meters, and 66 hectares at the farthest radius of 300-400 meters. Furthermore, in the Childhood age category (6-11 years old), the same movement pattern model was observed as the previous age category, but there were differences in the coverage area. In 2020, the potential coverage area started with 25 hectares at a radius of <100 meters, 75 hectares at 100-200 meters, 126 hectares at 200-300 meters, and 169 hectares at 300-400 meters. For 2019, the movement of the potential transmission area was lower at 298 hectares, with coverage of 19 hectares at a radius of <100 meters, 57 hectares at 100-200 meters, 94 hectares at 200-300 meters, and 129 hectares at 300-400 meters.

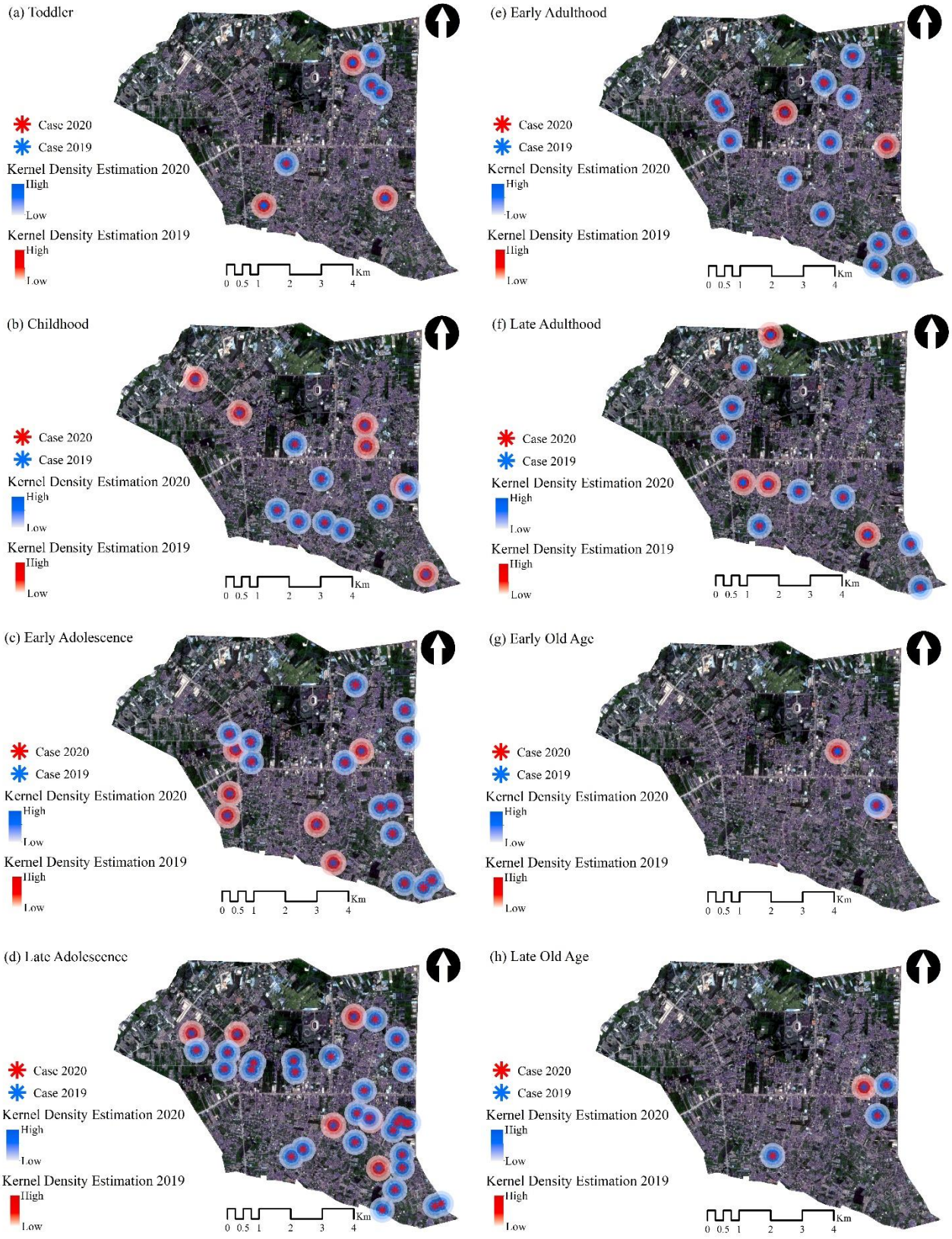

Figure 8. Kernel density estimation based on age category in 2019 and 2020

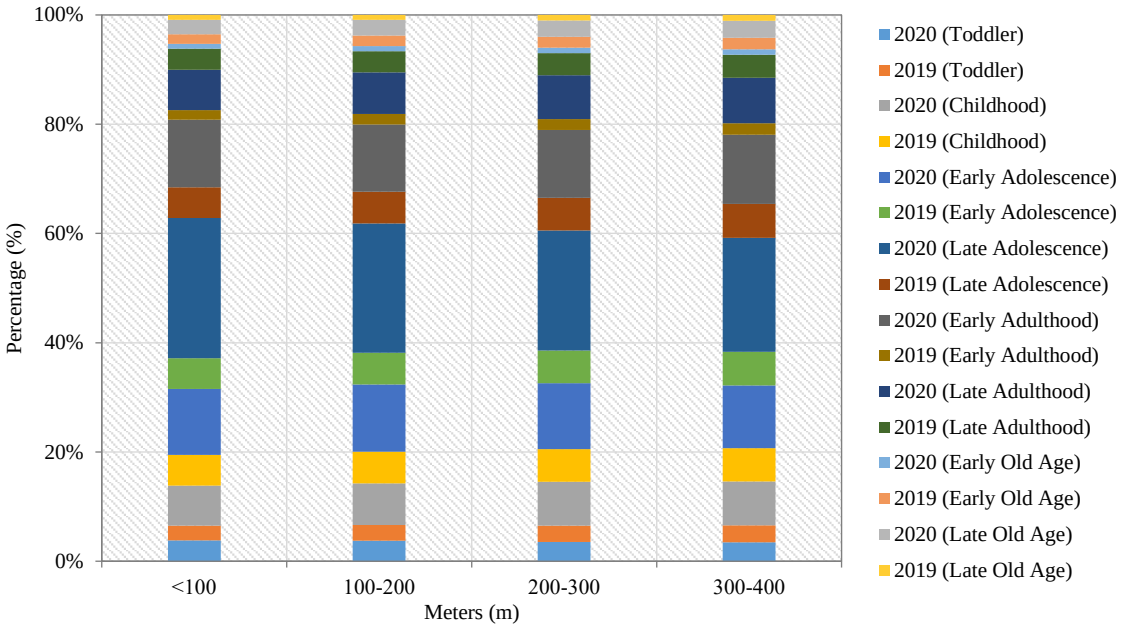

Figure 9. The percentage of DHF spread by age category in 2019 and 2020

In Early Adolescence (11-16 years), differences in movement patterns were observed compared to the two previous age categories. The movement was slightly initiated by transmission from the same vector, evidenced by a non-overlapping flight radius, preventing mutual influence or initiation from different sources. Regarding coverage at this age level, 41 hectares were recorded at a radius of <100 meters, 121 hectares at 100-200 meters, 189 hectares at 200-300 meters, and 243 hectares at the farthest radius of 300-400 meters in 2020. Compared to the potential coverage of the previous year, 19 hectares, 57 hectares, 94 hectares, and 129 hectares were found in the four radius categories namely <100 meters, 100-200 meters, 200-300 meters, and 300-400 meters respectively. This indicated that the coverage in 2019 was lower than in 2020. Additionally, in the Late Adolescence age category (17-25 years), the highest incidence of dengue fever was recorded with a four times increase observed from 302 hectares in 2019 to almost 1,104 hectares or 1.1 km^2 in 2020. At this age level, serious attention is needed to reduce the incidence rate, starting with vaccination or an ideal form of environmental protection easily adapted by the community.

In the Early Adulthood age category (26-35 years), which initially had two incidents, an increase to 14 incidents was observed. New transmission activities were found in this age group, increasing the potential area of transmission to 525 hectares. The changes in coverage area included 36 hectares at <100 meters, 102 hectares at 100-200 meters, 164 hectares at 200-300 meters, and 223 hectares at 300-400 meters, derived from the difference in potential area between both years. For the Late Adulthood age category (36-45 years old), a random transmission pattern with a systematic phenomenon was observed. An increase in potential transmission reaching an area of 200 hectares was recorded, with a distribution of radius coverage including 12 hectares at <100 meters around, 37 hectares at 100-200 meters, 63 hectares at 200-300 meters, and 88 hectares at 300-400 meters.

In the Early Old Age category (46-55 years), a decrease in the potential area reaching half of the previous year was observed throughout the entire radius of the potential range of transmission. This was attributed to the decrease in the incidence rate, approaching the absence of case findings throughout the observation period. Similar results were observed in the Late Old Age category (>55 years) with a less significant incidence rate but expanded area, reaching 100 hectares from the beginning of 2019 to the end of 2020. Subsequently, the entire site unit was subjected to a KDE approach, divided into two-year categories to analyze the density of *Aedes aegypti* mosquito infection in the observation area.

The estimated density for DHF transmission through the flight distance of *Aedes aegypti* mosquitoes is shown in Figure 5. The potential level of DHF transmission was denoted by a red overlay, indicating areas with high kernel density as the proximity of patients increased. This signifies a virus-

prone region where the red area is susceptible to dengue virus infection, potentially facilitating its transmission to the surroundings (Chen, 2018). Furthermore, the location of DHF cases correlated with the habitat of *Aedes aegypti* mosquitoes. Areas with close proximity to breeding sites are more prone to experiencing DHF incidence due to heightened susceptibility. Mitigating measures, such as closing water reservoirs, recycling or burying mosquito breeding items, and effectively managing drained reservoirs can help reduce the risk of transmission in these areas (Saita et al., 2022).

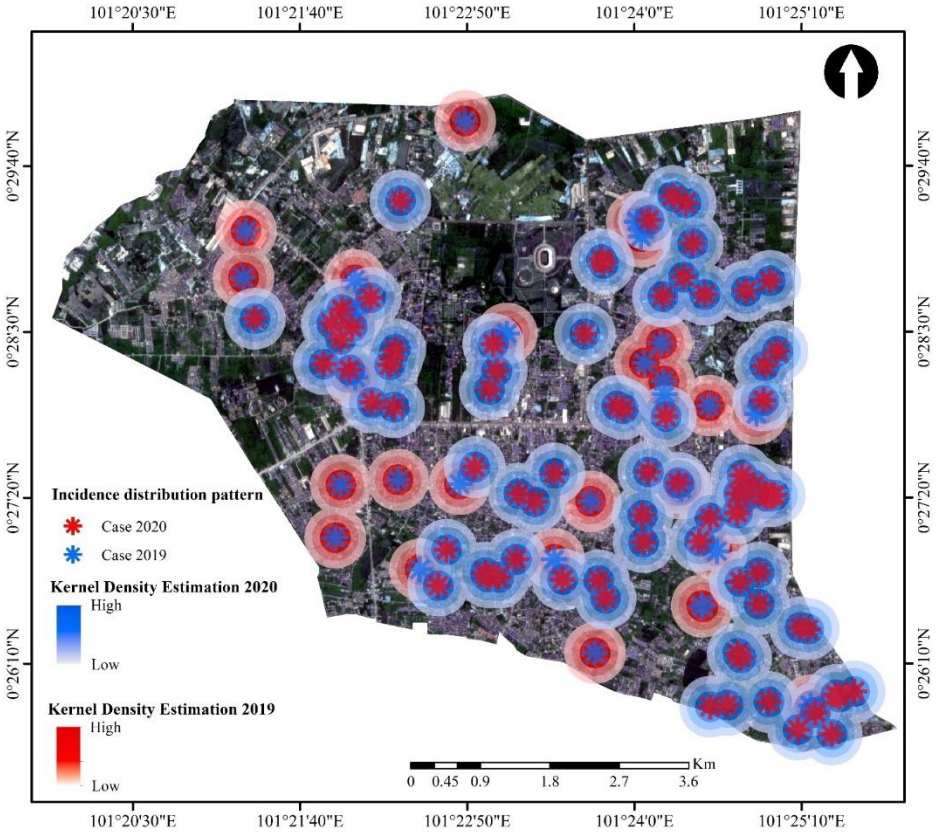

Figure 10. Kernel density estimation in 2019 and 2020

Based on the results of the validity assessment, a significant increase was observed based on the KDE approach, from 0.30% in 2019 to 0.63% in 2020, as shown in Table 2. The boundaries of areas with the potential for disease transmission, calculated considering geolocation, were closely related to the incidence data in the observation area. However, an increase in the number of DHF virus cases was observed. This was reflected in the number of DHF cases, with 30 reported in 2019 and 80 in 2020, showing an increase of 50 cases within one year.

Regarding patients affected by dengue hemorrhagic fever, when prevention and control measures are not swiftly initiated, the virus will spread more rapidly, potentially leading to death. Furthermore, this study found that poor environmental conditions and inadequate solid waste management result from the uncontrolled growth of urbanized areas, providing space for breeding sites. This factor is responsible for the indiscriminate disposal of plastic and bottle waste, forming pools suitable for the oviposition of *Aedes aegypti* mosquitoes (Souza et al., 2022).

Table 2. Assessment of the model in terms of validity

Description	Kernel Density Estimation	
	2020	2019
Potential of disease area (km^2)	22	13
Unpotential of disease area (km^2)	35	44
Validity (%)	0.63	0.30

This section discusses the areas affected by potential exposure to dengue virus bites from *Aedes aegypti* mosquitoes for one year. Based on the results, an increase was observed in the location of DHF cases in 2020. The potential area in 2019 was approximately 973.13 hectares, increasing to 1,572.36 hectares in 2020, as shown in Figure 6. Information related to the distance of the exposed zone was divided into four categories ranging from <100 meters, 100 to 200 meters, 200 to 300 meters, and 300 to 400 meters. As shown in Figure 11, the zone category of <100 meters had coverage of exposed area amounting to 53.14 hectares in 2019, which was higher compared to 2020, at 24,83 hectares. At a radius of 100-200 meters, the exposed area expanded, reaching 254.06 hectares in 2019 and 187.69 hectares in 2020. Extending to a larger radius of 200-300 meters in 2020, the area significantly increased to approximately 579.22 hectares, while in 2019, it was comparatively lower at 237.05 hectares. Finally, at the farthest radius of 300-400 meters, the increase in the number of cases in 2020 yielded the most significant area, reaching 780.62 hectares, compared to 2019, which had 428.88 hectares.

The distinction between each category corresponds to the distance from the location of the incident, estimating how far *Aedes aegypti* mosquitoes can fly without being disturbed by weather conditions and wind direction. The existence of broad categories of potential transmission zones was affected by the location of each patient acting as a host based on a high estimated kernel density. Additionally, areas with few or no cases of DHF were marked by color degradation, particularly faded red in the furthest zone from the flying distance of *Aedes aegypti* mosquitoes. Changes in land configuration, such as land use and urban development, including road networks and waste management systems directly or indirectly impact the transmission of dengue fever to the community (Andreo et al., 2021). The presence of excess water reservoirs also increases the abundance of mosquito vector species, creating suitable ecological spaces for the habitat and resulting in the potential for clustered transmission (Naqvi et al., 2021).

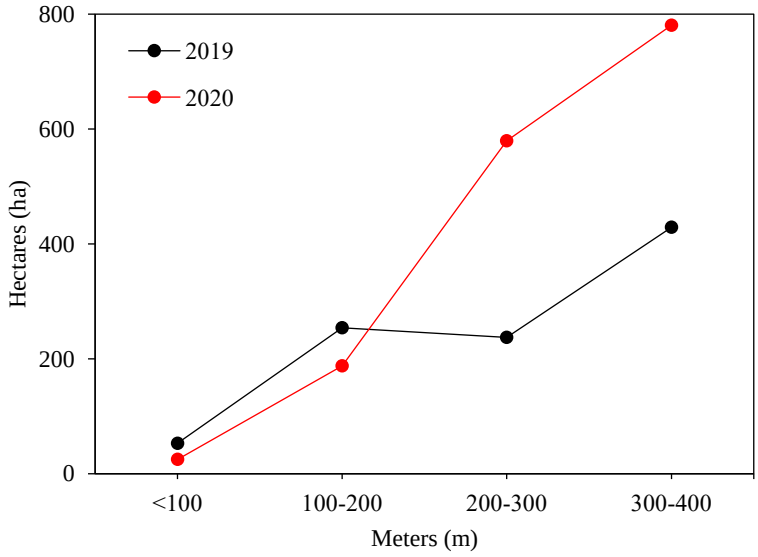

Figure 11. The curve of DHF spread in 2019 and 2020

The growth of new event points during the observation period in the designated area was illustrated by the utilization of the KDE approach. The estimation process algorithm for the pattern of changes in the incidence point was influenced by comparing to the existence of other events. The resulting interpretation suggests a significant increase in the number of incidence cases with the addition of an increasingly widespread potential transmission area. Furthermore, the development of anthropogenic activities in an area contributes to the potential presence of mosquito larvae and drives the demand for affordable health facilities, enhancing overall comfort in human living spaces. This in turn ensures community resilience in responding to *Aedes aegypti* mosquito outbreaks. The diversity of dengue virus transmission in the observation area was spatially influenced by complex interactions between humans and environmental factors of *Aedes aegypti* mosquitoes and climatology. In a particular phase,

climate anomalies influence the abundance of vector species, as well as the density and behavior of humans in the area. This was further compounded by high population and residential density, which reduced the distance between infected individuals, thereby accelerating transmission.

This study has certain limitations, such as not considering climate and other environmental variables. Incorporating these variables on a detailed scale could produce more complex zoning with a specific unit scale. This information is crucial for pinpointing locations expected to be part of the transmission area for *Aedes aegypti* mosquitoes. Special treatment is needed to understand how to anticipate dengue fever events in densely populated areas with building structures. In addition, it is necessary to build literacy about endemic outbreak mitigation in the community based on a sustainable environmental approach, coupled with the inclusion of climate change dynamics scenarios.

4. CONCLUSION

In conclusion, the analysis of DHF incidence using the nearest neighbor analysis and kernel density estimation (KDE) equation found distinct distribution patterns. The movement from random events to clustered groups underscored the impact of public awareness in maintaining clean conditions and prioritizing sanitation, hygiene, and drainage. This shift in distribution was indicative of improved community practices. Moreover, when estimating the transmission potential of *Aedes aegypti* mosquitoes based on the radius of the flight distance, weather conditions, and wind direction must be considered. Although this study observed a downward trend in the incidence of DHF, identifying potential areas of occurrence further reflected the history of vector control. The results obtained during the observation can be used to inform and guide future studies on environmental epidemiological ecology and the implementation of appropriate measures in disease control.

ACKNOWLEDGEMENTS

The authors are grateful to the Riau Province Health Office for granting permission to use surveillance data, as well as everyone who has reviewed and helped improve this paper.

CONFLICTS OF INTEREST

The authors declare that there is no conflict of interest regarding the publication of this manuscript.

ETHICAL APPROVAL

This study used secondary surveillance data, which included routine reports from (Riau Provincial Health Office) based on geospatial data containing geolocation information in the Tampan District area, Pekanbaru City. Therefore, the use of humans or animals as subjects of observation was unnecessary.

REFERENCES

Andreo V, Ximena P, Claudio G, Laura L, Carlos MS. Spatial distribution of *Aedes aegypti* oviposition temporal patterns and their relationship with environment and dengue incidence. Insects 2021;12(10):1-18.

Arifin, Niaz SM, Madey GR, Frank H, Collins. Spatial Agent-Based Simulation Modeling in Public Health. Canada: John Wiley and Sons, Inc; 2016.

Bansal SK, Karam VS, Sapna S, Sherwani MRK. Comparative larvicidal potential of different plant parts of *Withania somnifera* against vector mosquitoes in the semi-arid region of Rajasthan. Journal of Environmental Biology 2011;32(1):71-5.

Statistics of Pekanbaru Municipality (SoPM). Annual Report of Pekanbaru Municipality in Figures 2021. Pekanbaru: Statistics of Pekanbaru Municipality; 2021.

Chen WJ. Dengue outbreaks and the geographic distribution of dengue vectors in Taiwan: A 20-Year epidemiological analysis. Biomedical Journal 2018;41(5):283-9.

Devine, Gregor J, Michael J, Furlong. Insecticide use: Contexts and ecological consequences. Agriculture and Human Values 2007;(24):281-306.

Donthu, Naveen, Roland TR. Estimating geographic customer densities using kernel density estimation. Marketing Science 1989;8(2):191-203.

Ferraguti M, Martínez-de la Puente J, Brugueras S, Millet JP, Rius C, Valsecchi A, et al. Spatial distribution and temporal dynamics of invasive and native mosquitoes in a large Mediterranean city. Science of the Total Environment 2023;896:Article No. 165322.

Firdous, Jannathul, Ariza M, Muhammad AA, Muhamad I, Muhammad FI, et al. Knowledge, attitude and practice regarding dengue infection among Ipoh Community, Malaysia. Journal of Applied Pharmaceutical Science 2017;7(8):99-103.

Gatrell, Anthony C, Markku L. GIS and Health. Philadelphia: Taylor and Francis Inc; 2003.

Giofandi EA, Khursatul M, Kraugusteeliana K, Amira N, Cipta ES. The comparison of vector and raster data for the calculation of landscape environment using a geographic information system approach. IT Journal Research and Development 2023;7(2):209-19.

Hii, Yien L, Huaiping Z, Nawi N, Lee CN, Joacim R. Forecast of dengue incidence using temperature and rainfall. PLoS Neglected Tropical Diseases 2012;6(11):1-9.

King, Tania L, Rebecca JB, Lukar ET, Anne MK. Using kernel density estimation to understand the influence of neighbourhood destinations on BMI. BMJ Open 2016;6:1-8.

Lawson AB, Williams FLR. An introductory guide to disease mapping. American Journal of Epidemiology 2001; 154(9):881-2.

Liu, Wen H, Chen S, Ying L, Lei L, Chun QO. Epidemiological characteristics of imported acute infectious diseases in

Guangzhou, China, 2005-2019. PLoS Neglected Tropical Diseases 2022;16(12):1-12.

Lubinda, Jailos, Jesús ATC, Mallory RW, Adrian JM, Ahmad AHB, et al. Environmental suitability for *Aedes aegypti* and *Aedes albopictus* and the spatial distribution of major arboviral infections in Mexico. Parasite Epidemiology and Control 2019;6:e00116.

Masrani, Afiqah S, Nik RNH, Kamarul IM, Ahmad SY. Trends and spatial pattern analysis of dengue cases in Northeast Malaysia. Journal of Preventive Medicine and Public Health 2022;55(1):80-7.

Molina G, Licet P, Lina AGB, Leonardo ARO. Models of spatial analysis for vector-borne diseases studies: A systematic review. Veterinary World 2022;15(8):1975-89.

Murray, Natasha EA, Mikkel BQ, Annelies WS. Epidemiology of dengue: Past, present and future prospects. Clinical Epidemiology 2013;5(1):299-309.

Naqvi, Syed AA, Muhammad S, Liaqat AW, Shoaib K, Saima S, et al. Integrating spatial modelling and space-time pattern mining analytics for vector disease-related health perspectives: A case of dengue fever in Pakistan. International Journal of Environmental Research and Public Health 2021;18(22):1-30.

Negev, Maya, Shlomit P, Alexandra C, Noemie GPO, Uri S, et al. Impacts of climate change on vector borne diseases in the Mediterranean Basin — Implications for preparedness and adaptation policy. International Journal of Environmental Research and Public Health 2015;12(6):6745-70.

Portella, Tatiana P, Roberto AK. Spatial–Temporal pattern of cutaneous leishmaniasis in Brazil. Infectious Diseases of Poverty 2021;10(1):1-11.

Ragab, Sanad H, Mostafa AK, Riham HT, Mohamed ET. Spatial distribution of appropriate aquatic mosquitos' larval sites occurrence using integration of field data and GIS techniques. Egyptian Journal of Aquatic Biology and Fisheries 2023;27(4):355-71.

Ramadona, Aditya L, Yesim T, Jonas W, Lutfan L, Adi U, et al. Predicting the dengue cluster outbreak dynamics in Yogyakarta, Indonesia: A modelling study. The Lancet Regional Health - Southeast Asia 2023;15:1-8.

Rushton G. Public health, GIS, and spatial analytic tools. Annual Review of Public Health 2003;24:43-56.

Saita, Sayambhu, Sasithan M, Tassanee S. Temporal variations and spatial clusters of dengue in Thailand: Longitudinal study before and during the coronavirus disease (COVID-19) pandemic. Tropical Medicine and Infectious Disease 2022;7(8):1-14.

Satoto TBT, Nur AP, Wida P, Hari KJ, Purwono, Rumbiwati, et al. Occurrence of natural vertical transmission of Zika like virus in *Aedes aegypti* mosquito in Jambi City. Kesmas: National Public Health Journal 2019;13(4):189-94.

Sekarrini CE, Sumarmi, Syamsul B, Didik T. Fuzzy set model of dengue using imageries and the geographic information system in Palembang. International Journal of Innovation, Creativity and Change 2020;13(10):1264-93.

Sekarrini CE, Sumarmi S, Syamsul B, Didik T, Eggy AG. The application of geographic information system for dengue epidemic in Southeast Asia: A review on trends and opportunity. Journal of Public Health Research 2022a; 11(3):1-6.

Sekarrini CE, Syamsul B, Didik T, Giofandi EA. Spatial temporal analysis of dengue hemorrhagic fever occurrence (Case study of Palembang City, South Sumatera Province, Indonesia). Malaysian Journal of Medical Sciences 2022b;18(17):39-45.

Setiawati MD. The effect of climate variables on dengue Burden in Indonesia: A case study from Medan City. Journal of Geoscience and Environment Protection 2019;7(10):80-94.

Shi X. Selection of bandwidth type and adjustment side in kernel density estimation over inhomogeneous backgrounds. International Journal of Geographical Information Science 2010;24(5):643-60.

Souza SJP, André CG, Nildimar AH, Daniel CPC, Natali MS, Sarita TM, et al. Spatial and temporal distribution of *Aedes aegypti* and *Aedes albopictus* oviposition on the Coast of Paraná, Brazil, a recent area of dengue virus transmission. Tropical Medicine and Infectious Disease 2022;7(9):1-14.

Spencer J, Gustavo A. Kernel density estimation as a technique for assessing availability of health services in Nicaragua. Health Services and Outcomes Research Methodology 2007;7: 145-57.

Sun Q, Sijie W, Kaiqi Z, Fei M, Xiaozhuang G, Tingzhen L. Spatial pattern of urban system based on gravity model and whole network analysis in eight urban agglomerations of China. Mathematical Problems in Engineering 2019;2019: Article No. 6509726.

Verdonschot PFM, Anna ABL. Flight distance of mosquitoes (culicidae): A metadata analysis to support the management of barrier zones around rewetted and newly constructed wetlands. Limnologica 2014;45:69-79.

Waller LA, Carol AG. Applied Spatial Statistics for Public Health Data. New Jersey, United States: John Wiley and Sons, Inc; 2004.

Wang Z, Lin L, Hanlin Z, Minxuan L. How is the confidentiality of crime locations affected by parameters in kernel density estimation? ISPRS International Journal of Geo-Information 2019;8(12):1-12.

Wijayanti SPM, Thibaud P, Margo CT, Stephanie MR, Melanie M, Esther S, et al. The importance of socio-economic versus environmental risk factors for reported dengue Cases in Java, Indonesia. PLoS Neglected Tropical Diseases 2016; 10(9):1-15.

Zhang Y, Lei W, Guozhen W, Jiabao X, Tianxing Z. An ecological assessment of the potential pandemic threat of dengue virus in Zhejiang Province of China. BMC Infectious Diseases 2023;23(473)1-10.